



Original article

CeFe nanofibrous carbon nanozyme integrated with smartphone for the point-of-care testing of norfloxacin in water

Yue Liu ^{a, b}, Taimei Cai ^{a, *}, Sen Chen ^b, Tao Wen ^c, Hailong Peng ^{b, **}^a Key Laboratory of Natural Microbial Medicine Research of Jiangxi Province, School of Life Science, Jiangxi Science and Technology Normal University, Nanchang, 330013, China^b School of Chemistry and Chemical Engineering, Nanchang University, Nanchang, 330031, China^c College of Mechanical and Intelligent Manufacturing, Central South University of Forestry and Technology, Changsha, 410004, China

ARTICLE INFO

Article history:

Received 26 March 2024

Received in revised form

3 June 2024

Accepted 22 June 2024

Available online 26 June 2024

Keywords:

CeO₂ nanoparticles

Peroxidase-like activity

Nanofibrous carbon microspheres

Point-of-care testing

Norfloxacin

ABSTRACT

The overuse of antibiotics has led to the severe contamination of water bodies, posing a considerable hazard to human health. Therefore, the development of an accurate and rapid point-of-care testing (POCT) platform for the quantitative detection of antibiotics is necessary. In this study, Cerium oxide (CeO₂) and Ferrosioferric oxide (Fe₃O₄) nanoparticles were simultaneously encapsulated into N-doped nanofibrous carbon microspheres to form a novel nanozyme (CeFe-NCMzyme) with a porous structure, high surface area, and N-doped carbon material properties, leading to a considerable enhancement of the peroxidase (POD)-like activity compared with that of the CeO₂ or Fe₃O₄ nanoparticles alone. The POD-like activity of CeFe-NCMzyme can be quenched using L-Cysteine (Cys) and subsequently restored by the addition of a quinolone antibiotic (norfloxacin, NOR). Therefore, CeFe-NCMzyme was used as a colorimetric sensor to detect NOR via an “On-Off” model of POD-like activity. The sensor possessed a wide linear range of 0.05–20.0 μM ($R^2 = 0.9910$) with a detection limit of 35.70 nM. Furthermore, a smartphone-assisted POCT platform with CeFe-NCMzyme was fabricated for quantitative detection of NOR based on RGB analysis. With the use of the POCT platform, a linear range of 0.1–20.0 μM and a detection limit of 54.10 nM were obtained. The spiked recoveries in the water samples were ranged from 97.73% to 102.01%, and the sensor exhibited good accuracy and acceptable reliability. This study provides a portable POCT platform for the on-site and quantitative monitoring of quinolone antibiotics in real samples, particularly in resource-constrained settings.

© 2024 The Author(s). Published by Elsevier B.V. on behalf of Xi'an Jiaotong University. This is an open access article under the CC BY-NC-ND license (<http://creativecommons.org/licenses/by-nc-nd/4.0/>).

1. Introduction

Quinolones are considered as a critically important antibiotic owing to their therapeutic multipurpose characteristics [1]. Quinolone antibiotics (QN) have been widely applied as clinical, anti-infective, and veterinary antimicrobials [2]. QN residues have been detected in aquatic environments, and their presence leads to the development of antibiotic-resistant bacteria and antibiotic-resistant genes, consequently posing a potential hazard to human health and the ecosystem [3]. Therefore, the development of a sensitive and rapid detection strategy for QN residues plays a vital

role in the monitoring of QN contamination in aquatic environments and the protection of human health.

Conventional methods, such as high-performance liquid chromatography (HPLC) [4], mass spectrometry (MS) [5], and liquid chromatography-MS (LC-MS) [6], are the standard methods employed for QN detection in laboratories. These methods yield excellent results with high precision and sensitivity. However, their application in resource-constrained areas is severely limited by several drawbacks, including expensive laboratory equipment, time-consuming, complex sample-preparation procedures, and the requirement of skilled operators [7]. To address the aforementioned challenges associated with instrumentation methods, the fabrication of a quantitative point-of-care testing (POCT) system for real-time and rapid detection of QN is necessary. POCT is an inexpensive and rapid analytical method that eliminates the requirement for expensive equipment, and skilled operators, and reduces testing costs and mismanagement [8]. POCT methods have been applied in

Peer review under responsibility of Xi'an Jiaotong University.

* Corresponding author.

** Corresponding author.

E-mail addresses: 1020220503@jxstnu.edu.cn (T. Cai), penghailong@ncu.edu.cn (H. Peng).

health management, disease diagnosis, environmental monitoring, and food safety [9], particularly in resource-limited areas [10]. Optical analysis is considered a candidate technique for POCT because of its rapid response, high sensitivity, convenience of use, and on-site operation [11]. Among the optical methods, the colorimetric assay has received substantial attention in field of detection because of its advantages of power-free and straightforward readout signals manifested by simple colour changes, offering a promising method for easy-to-use POCT devices and on-site detection via naked-eyes [12]. However, POCT with naked-eyes detection can currently only provide a qualitative assessment, failing to offer a precise quantitative appraisal of the residue level [13]. Moreover, the naked-eyes detection is generally limited by its relatively low sensitivity and difficulty in distinguishing the slight colour changes at low levels [14]. Therefore, the POCT platform should be combined with miniaturized device to realize a rapid “sample-in-answer-out” system and improve detection accuracy.

Among miniaturized devices, smartphones have the potential to achieve accurate quantification to realize high-performance POCT due to their portability, built-in camera functions, and other simple opto-mechanical components [15]. Owing to their advantages of high-resolution image acquisition, excellent data-processing and transferring capabilities, and wireless connectivity, smartphones are considered as cost-effective, rapid, easy-to-use, and portable devices for the construction of POCT platforms without the assistance of other complex equipment and laboratories [16]. Thus far, several smartphone-based POCT platforms integrated with colorimetric materials, such as quantum dots [17], carbon-based nanomaterials [18], metal-organic frameworks (MOFs) [19], and nanozymes [20], have been developed for application in clinical medical and detection fields. Among colorimetric materials, nanozymes have emerged as promising materials for application in POCT [21] owing to their advantages of tuneable enzyme-like activity, low cost, multifunctionality, and good stability and versatility [21,22].

CeO₂ nanoparticles (CeO₂ NPs) are efficient nanozymes with high mimicking activity owing to their high thermal stability, Ce⁴⁺/Ce³⁺ redox potential property, and tuneable electronic capability [23]. Furthermore, CeO₂ NPs have abundant oxygen vacancies and surface-active groups, which are beneficial for their catalytic-like activity [24]. However, CeO₂ NPs are limited by issues related to their aggregation caused by their relatively high surface energy, which decreases their catalytic activity [23]. Additionally, CeO₂ NPs can only operate under relatively harsh conditions such as high temperatures (≥ 70 °C) and long durations (≥ 60 min) [25]. To overcome these disadvantages, Ce-based MOFs have attracted considerable attention in the field of enzyme mimics due to their large surface areas, high stability, unsaturated metal sites, and the well-defined clusters [26]. However, MOF supports have several drawbacks, such as expensive, multiple and complicated preparation processes, and time-consuming [27]. Recently, N-doped carbon materials with rich pore structures have been recognized as promising candidates for catalyst supports [28]. The loading of CeO₂ NPs onto N-doped porous carbon materials mitigates aggregation issues and forms a heterogeneous structure, which facilitates the effective separation of electron and hole pairs, promoting electron transfer and catalytic activity [29]. Furthermore, the catalytic efficiency of CeO₂ NPs also can be improved by creating additional oxygen vacancies via different methods, such as replacing a portion of Ce in the ceria lattice with cations possessing an appropriate radius [30]. A large number of oxygen vacancies can be formed by doping of Fe³⁺ into CeO₂ NPs, which reduces the band gap, leading to an improvement in the catalytic efficiency of CeO₂ NPs. However, the internal magnetism and van der Waals forces may cause the accumulation of nanosized Fe₃O₄, possibly affecting catalytic efficiency of the Fe₃O₄/CeO₂ composite [31]. Therefore, the incorporation of

Fe₃O₄/CeO₂ NPs into supporting materials is an effective method for overcoming the aforementioned issues. To the best of our knowledge, the simultaneous incorporation of CeO₂ and Fe₃O₄ NPs into N-doped nanofibrous carbon microspheres with a hierarchical porous architecture to form a nanozyme for improving catalytic efficiency has not been yet reported thus far.

Inspired by the abovementioned factors, CeO₂ NPs were synthesized and loaded into N-doped nanofibrous carbon microspheres along with Fe₃O₄ NPs to form a nanozyme (CeFe-NCMzyme). Owing to the combination of the advantageous properties of CeO₂, N-doped carbon materials and Fe₃O₄, CeFe-NCMzyme displayed considerably enhanced peroxidase (POD)-like activity compared with CeO₂ NPs or Fe₃O₄ NPs. Therefore, CeFe-NCMzyme was used as a colorimetric sensor for QN detection (norfloxacin (NOR)) via “on-off” effects on the POD-like activity. Furthermore, a quantitative POCT platform for the rapid and on-site detection of NOR was developed by combining a smartphone with CeFe-NCMzyme. NOR concentration-dependent colour photographs were captured and transformed to digital B/G values using the POCT platform. By plotting the digital B/G values versus NOR concentration, rapid and on-site visual quantification of NOR in water and drug samples can be realized via the POCT platform. Clearly, CeFe-NCMzyme-based methods for QN detection offer the advantages of being low-cost, expensive-instrument-free, and rapidness.

2. Materials and methods

2.1. Materials and reagents

Chitin was purchased from Golden-Shell Biochemical Co., Ltd. (Yuhuan, Zhejiang, China). 3,3',5,5'-tetramethylbenzidine (TMB), L-Cysteine (Cys), norfloxacin, erythromycin, terramycin hydrochloride, doxycycline hydrochloride, and sodium acetate anhydrous were all purchased from Macklin Biochemical Co., Ltd. (Shanghai, China). Urea was purchased from Sigma-Aldrich Co., Ltd. (Shanghai, China). Tert-Butanol and 2,2,4-Trimethylpentane were purchased from Damao Chemicals Reagent Factory Co., Ltd. (Tianjin, China). Fe₃O₄ nanoparticles (99%, 20 nm), Span 85, and Tween 85 were obtained from Aladdin Biochemical Technology Co., Ltd. (Shanghai, China). Cerium(III) nitrate hexahydrate, hydrogen peroxide (H₂O₂; 30% (w/w)), ammonia water (NH₃·H₂O; 25%–28%), glycol, alcohol, and D-Glucose were all bought from Xilong Co., Ltd. (Guangzhou, China).

2.2. Characterizations of CeFe-NCMzyme

The absorption spectra of CeFe-NCMzyme was determined by UV-vis spectra (UV-1900, Puxi General Instrument Co., Ltd., Beijing, China). The morphology and elements of CeFe-NCMzyme were determined using the scanning electron microscope (SEM; Sigma 300, Oberkochen, Germany). The phase structure of CeFe-NCMzyme was determined by X-ray diffraction (XRD; Bruker D8 Advance, Karlsruhe, Germany). X-ray photoelectron spectroscopy (XPS; Thermo Scientific K-Alpha, Billerica, MA, USA) was used to characterize the composition of CeFe-NCMzyme. Free radicals in the CeFe-NCMzyme system were tested by electron spin resonance (ESR; Bruker EMXplus, Karlsruhe, Germany).

2.3. Synthesis of CeO₂ NPs

Glycol (120 mL), deionized water (10 mL), and NH₃·H₂O (3 mL) were added successively into a round-bottomed flask and mixed at 60 °C for 10 min. After the reaction, dopamine hydrochloride (10 mL, 50 mg/mL) was added into the mixture solution. Then, Ce(NO₃)₃·6H₂O (3 mL, 33.3 mg/mL) was dropped into the mixture solution and kept in an oil bath at 60 °C for 12 h. The reaction

solution was centrifuged and washed with a mixture of ethanol/water for three times. After that, the obtained product was freeze-dried for 12 h. The freeze-dried samples were transformed to a tube furnace and heated to 900 °C at 5 °C/min and kept at 900 °C for 3 h. Finally, the obtained CeO₂ NPs were cooled to room temperature under nitrogen condition.

2.4. Synthesis of CeFe-NCMzyme

The purified chitin powder (6 g) was dispersed into a NaOH/urea/water (11:4:85, *m/m/m*) solution (94 g) with rapidly stirring for 10 min. The solution was frozen at −30 °C for 4 h, and then thawed at room temperature. After three freeze-thaw cycles, Fe₃O₄ NPs (0.6 g) and CeO₂ NPs (0.4 g) were added into the chitin solution with stirring for 2 min to obtain a water phase. The oil phase was obtained by stirring of Span 85 (4.4 g) and isooctane (100 g) at 0 °C for 30 min. Then, the water phase was added into the oil phase within 5 min and vigorously stirred for 60 min to obtain emulsion solution. After that, Tween 85 (2.4 g) was added into the emulsion with stirring for another 60 min. The emulsion was then stirred in a water bath at 60 °C for 5 min and adjusted pH to 7 using HCl (10%, *V/V*). After that, the emulsion was soaked in tert-butanol for 6 h, frozen using liquid nitrogen, and rapidly dried in a vacuum freeze dryer for 24 h. Finally, the dried sample was carbonized at 650 °C for 2 h at a rate of 3 °C/min. The CeFe-NCMzyme can be obtained after cooling to room temperature.

2.5. Catalytic property of CeFe-NCMzyme

The POD-like activity of CeFe-NCMzyme was evaluated by UV-vis spectra at 652 nm. TMB (100 μL, 10 mM), H₂O₂ (200 μL, 200 mM), and CeFe-NCMzyme (30 μL, 1 mg/mL) were added into HAc-NaAc buffer solution (1,670 μL, 0.1 M, pH = 3.5) and reacted at 35 °C for 10 min. The steady-state kinetics of TMB and H₂O₂ were investigated by adjusting different concentrations of TMB or H₂O₂, and the kinetic values were obtained via the steady-state kinetics and Michaelis–Menten equations:

$$v = \frac{V_{\max}[S]}{K_M + [S]} \quad (1)$$

$$\frac{1}{v} = \frac{K_M}{V_{\max}[S]} + \frac{1}{V_{\max}} \quad (2)$$

where v and K_M is the initial reaction velocity and the Michaelis constant, respectively. $[S]$ is the concentration of TMB or H₂O₂ substrate. V_{\max} is the maximal velocity at the saturate substrate concentration.

2.6. Colorimetric detection of NOR using CeFe-NCMzyme

Firstly, the concentration of Cys for NOR detection was optimized. H₂O₂ (200 μL, 200 mM), TMB (100 μL, 10 mM) and CeFe-NCMzyme (30 μL, 1 mg/mL) were mixed with HAc-NaAc buffer solution (pH = 3.5, 0.1 M), and different Cys concentrations were added into the buffer solution to keep the total volume at 2 mL. The reaction was carried out at 35 °C for 10 min and the peak (652 nm) was detected by UV-vis. For NOR detection, different NOR concentrations and the optimized Cys were mixed with acetic acid buffer (0.1 M, pH = 3.5) containing CeFe-NCMzyme (30 μL, 1 mg/mL), TMB (100 μL, 10 mM), and H₂O₂ (200 μL, 200 mM). The total volume was maintained 2 mL. After reaction for 10 min at 35 °C, the peak (652 nm) was detected via UV-vis.

2.7. Determination of NOR in real samples using CeFe-NCMzyme

Water samples (Ganjiang River water, Poyang Lake water from four different areas, tap water, and purified water) were filtered with filter paper and microporous filter, respectively. The NOR content in the actual water sample was analyzed by the spiking method with concentrations of 5 μM, 50 μM, and 150 μM. Spiked sample (200 μL) and the optimized Cys were mixed with acetic acid buffer (0.1 M, pH = 3.5) containing CeFe-NCMzyme (30 μL, 1 mg/mL), TMB (100 μL, 10 mM), and H₂O₂ (200 μL, 200 mM) to maintain the total volume of 2 mL. After reaction for 10 min at 35 °C, the absorption at 652 nm was performed via UV-vis spectra. The selectivity of CeFe-NCMzyme was investigated using oxytetracycline, erythromycin, doxycycline, histidine, aspartic acid, alanine, glycine, Mn²⁺, Na⁺, Ca²⁺, Ni²⁺, Zn²⁺, and L-Cys as interferents. CeFe-NCMzyme solution was stored at 4 °C and its POD-like activity was evaluated within two months for evaluation its stability.

2.8. Detection of NOR using POCT platform

Different NOR concentrations were added into the CeFe-NCMzyme + H₂O₂ + TMB + Cys system. After 10 min of reaction at 35 °C, the color images were captured using the digital camera inside a smartphone. Subsequently, the obtained images were analyzed by the ColorPicker App and immediately converted into red, green, and blue (RGB) values. The linear relationship between blue-to-green (B/G) values and NOR concentrations was plotted for performing the real-time and rapid quantitative readout of NOR in real samples.

3. Results and discussion

3.1. Characterization

Evaluation of the morphology of CeFe-NCMzyme via SEM (Figs. 1A–C) demonstrated that it possessed a spherical shape with a porous structure and was composed of carbon nanofibers. The elemental distribution results of CeFe-NCMzyme are presented in Figs. 1D–H, clearly depicting that C, N, O, Fe, and Ce elements were uniformly distributed in CeFe-NCMzyme. The N adsorption/desorption experimental results showed that CeFe-NCMzyme exhibited a type I H3 hysteresis loop (Fig. 1I) with a substantially large specific surface area (304.70 m²/g) and a hierarchical porous architecture. Fig. 1J showed the XRD patterns of CeO₂ NPs and CeFe-NCMzyme, indicating that CeO₂ NPs exhibited a cubic fluorite structure, as suggested by the presence of (111), (200), (220), (311), (222), (400), and (331) peaks (JCPDS card No. 34-0394) [32]. Furthermore, similar peaks were observed for CeFe-NCMzyme, illustrating that the fluorite structure of CeO₂ NPs remained unchanged after loading into CeFe-NCMzyme along with Fe₃O₄. However, the peak intensity of CeO₂ NPs was substantially weakened in CeFe-NCMzyme pattern, which may be owing to the replacement of Ce⁴⁺ by Fe³⁺ CeO₂ [32]. Furthermore, the small peaks at 35.37° are attributed to Fe₃O₄ (311) (JCPDS No. 26-1136). Additionally, the two peaks at 23.71° and 45.13° corresponded to the (002) and (100) crystal planes of the carbon nanofiber and originated from the amorphous carbon and graphitic carbon, respectively. The magnetic properties of CeFe-NCMzyme were evaluated using a vibrating sample magnetometer (VSM) (Fig. S1). The magnetic hysteresis loop curves indicated negligible hysteresis and zero coercivity with a saturation magnetization value of 22.36 emu/g. These results confirmed the successful preparation of CeFe-NCMzyme with a hierarchical porous architecture and large surface area.

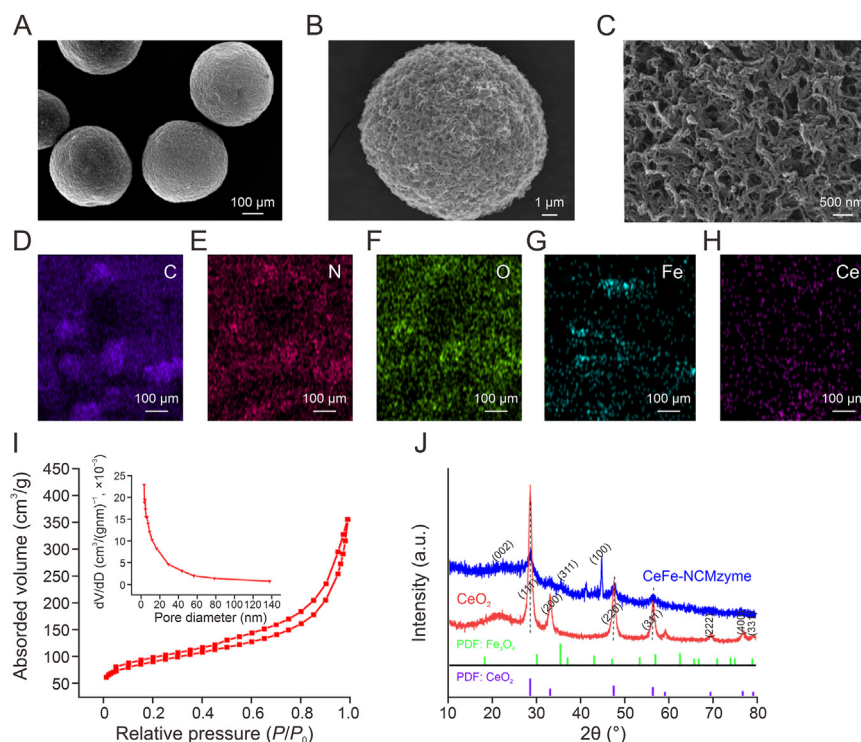


Fig. 1. Characterizations of CeFe-NCMzyme. (A–C) scanning electron microscope (SEM), (D–H) mapping, (I) nitrogen adsorption-desorption isotherm and pore size distribution of CeFe-NCMzyme, and (J) X-ray diffraction (XRD) patterns of CeFe-NCMzyme and CeO₂.

3.2. Enzyme-like catalytic activity of CeFe-NCMzyme

The POD-like activity of CeFe-NCMzyme was evaluated using TMB as the chromogenic substrate. As shown in Fig. 2A, the colour remained unchanged and no absorption peak was observed at 652 nm for the TMB + H₂O₂ system. The colour changed slightly with the appearance of a small peak at 652 nm for CeFe-NCMzyme + TMB system, indicating that CeFe-NCMzyme had weak oxidase-like activity. Notably, the colour rapidly changed from colourless to blue with the appearance of a strong absorption peak at 652 nm for CeFe-NCMzyme + TMB + H₂O₂ system (Fig. 2A), illustrating that CeFe-NCMzyme possessed a strong POD-like activity. To confirm the enhancement of POD-like activity, the absorption at 652 nm was investigated for different systems, namely, CeFe-NCMzyme + TMB + H₂O₂, CeO₂ NPs + TMB + H₂O₂, and Fe₃O₄ NPs + TMB + H₂O₂ (Fig. 2B). Clearly, the peak intensity of CeFe-NCMzyme was approximately 1.70- and 15-folds higher than those of CeO₂ NPs and Fe₃O₄ NPs, respectively. The blue colour of CeFe-NCMzyme is darker than that of CeO₂ NPs and Fe₃O₄ NPs (Fig. 2B inset). Furthermore, Fig. 2B revealed that the peak intensity of CeFe-NCMzyme was substantially higher than that of Fe-NCMzyme. These results demonstrated that the POD-like activity of CeFe-NCMzyme was considerably higher than the combined activities of CeO₂ NPs and Fe₃O₄ NPs, which was because of the synergistic effect of the nanocomposites, N-doped carbon materials, and large surface area.

The optimal conditions for the POD-like activity of CeFe-NCMzyme were investigated by changing various parameters, including temperature, pH, and CeFe-NCMzyme concentration (Fig. S2). Clearly, CeFe-NCMzyme exhibited a high POD-like activity over a broad pH range of pH 2–5 and a temperature range of 25–60 °C (Fig. S2A and B). The highest POD-like activity was

observed at an optimal pH of 3.5, and temperature of 35 °C. Fig. S2C depicted a rapid increase in the absorbance with an increase in CeFe-NCMzyme concentration from 1 μg/mL to 15 μg/mL. A relatively smooth change was observed when CeFe-NCMzyme concentration exceeded 15 μg/mL, which was considered as the optimal nanozyme concentration. Under the optimal conditions, the classical Michaelis-Menten and Lineweaver-Burk models were applied to fit the results obtained for the CeFe-NCMzyme + TMB + H₂O₂ system (Figs. 2C–F). V_{\max} and K_M values were calculated using the Michaelis-Menten equation. The K_M and V_{\max} values were 9.246 mM and 13.75×10^{-8} M/s for H₂O₂ and 0.379 mM and 8.396×10^{-8} M/s for TMB (Table S1), respectively. Compared with horseradish peroxidase (HRP) [33], the K_M value of CeFe-NCMzyme for TMB was lower than that of HRP (0.434 mM), indicating that CeFe-NCMzyme possessed a higher affinity for TMB than that of HRP. Meanwhile, the V_{\max} value of CeFe-NCMzyme for H₂O₂ was higher than that of HRP (8.71×10^{-8} M/s). A lower K_M value implies a higher enzyme affinity for the substrate, and a higher V_{\max} value indicates the higher catalytic efficiency. Therefore, CeFe-NCMzyme exhibited excellent POD-like activity.

3.3. POD-like catalytic mechanism of CeFe-NCMzyme

To investigate the catalytic mechanism, the chemical valence states of the constituent elements in CeO₂ NPs and CeFe-NCMzyme were evaluated via XPS experiment. The Ce 3d spectra of CeO₂ NPs (Fig. 3A) consist of eight peaks originating from the spin-orbit coupling of 3d_{5/2} and 3d_{3/2} orbitals [34]. The peaks at 888.79 eV, 898.15 eV, 882.25 eV, and 885.08 eV were attributed to the 3d_{5/2} orbitals, whereas those at 900.81 eV, 907.28 eV, 902.67 eV, and 916.54 eV corresponded to the 3d_{3/2} orbitals. The peaks at 898.15 eV, 882.25 eV, and 885.08 eV in the 3d_{5/2} orbitals and those

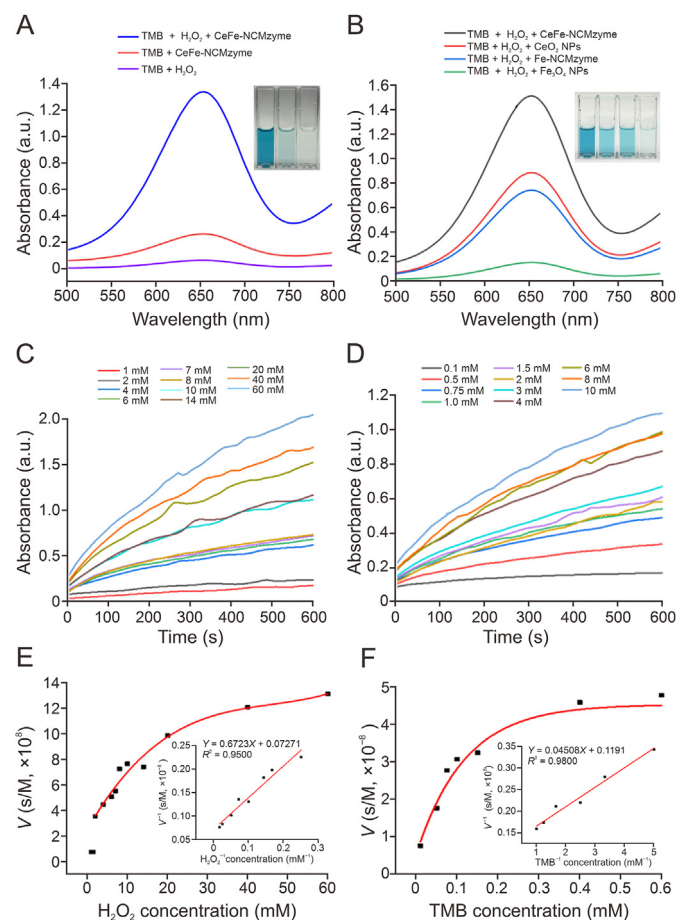


Fig. 2. Peroxidase (POD)-like activity and steady-state kinetic of CeFe-NCMzyme. (A) Comparison of POD-like activity of 3,3',5,5'-tetramethylbenzidine (TMB) + CeFe-NCMzyme, TMB + H₂O₂, and TMB + H₂O₂ + CeFe-NCMzyme systems. (B) Comparison of POD-like activity of TMB + H₂O₂ + CeFe-NCMzyme, TMB + H₂O₂ + Fe₃O₄ NPs, TMB + H₂O₂ + CeFe-NCMzyme, and TMB + H₂O₂ + CeO₂ NPs systems (inset is corresponding photos), and (C–F) Steady-state kinetic of CeFe-NCMzyme. NPs: nanoparticles.

at 900.81 eV, 907.28 eV, and 916.54 eV in the 3d_{3/2} orbitals were caused by Ce⁴⁺. The remaining peaks, namely, those at 885.08 eV and 902.67 eV originating from the 3d_{5/2} and 3d_{3/2} orbitals, respectively, were assigned to Ce³⁺. These observations confirmed the presence of both ions of Ce⁴⁺ and Ce³⁺ ions in the CeO₂ ceria lattice. Moreover, Fig. 3A demonstrated that the peak area of Ce⁴⁺ was higher than that of Ce³⁺, which implies that the content of Ce⁴⁺ (81.82%) was higher than that of Ce³⁺ (18.18%). After loading into CeFe-NCMzyme, the corresponding peaks of Ce³⁺ and Ce⁴⁺ remained in the XPS spectra (Fig. 3B), and the Ce³⁺ content notably increased from 18.18% to 48.23%. These results can be attributed to the presence of N-doped carbon nanofibers and iron atoms, which are beneficial for the reducing of Ce⁴⁺ to Ce³⁺ with production of oxygen vacancies after carbonization. Clearly, the number of oxygen vacancies increased with increasing of Ce³⁺ content in CeFe-NCMzyme. To further confirm the increase in the number of oxygen vacancies, the deconvolution of O1s XPS spectra was also performed (Fig. 3C). The peak at 531.58 eV can be attributed to the oxygen vacancies for CeO₂ with a content of 35.45%. After loading into CeFe-NCMzyme, the peak intensity of oxygen vacancies increased with an increase in content to 38.79% (Fig. 3D). Generally, oxygen vacancies can serve as electron traps to improve their electron transfer [35]. Furthermore, oxygen vacancies can promote the adsorption performance of substrates and subsequently

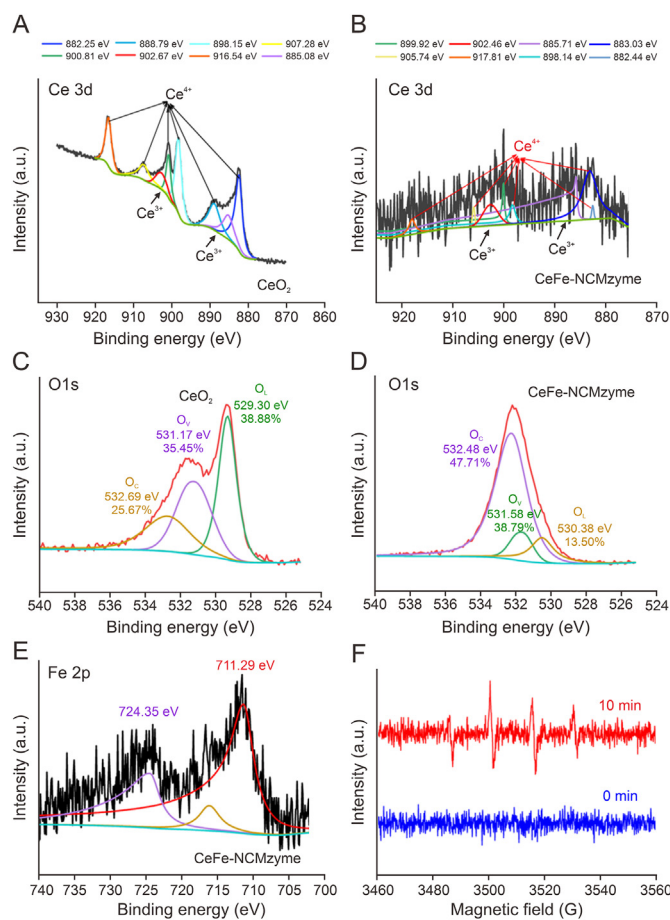
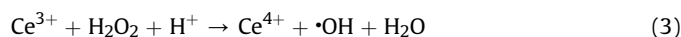
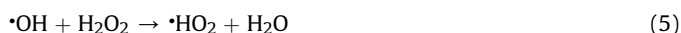


Fig. 3. X-ray photoelectron spectroscopy (XPS) of CeO₂ and CeFe-NCMzyme. (A, B) Ce 3d spectrum, (C, D) O 1s spectrum, (E) Fe 2p spectrum, and (F) electron paramagnetic resonance (EPR) of CeFe-NCMzyme.

improve the catalytic activity. Therefore, the catalytic activity of CeO₂ was improved after loading into CeFe-NCMzyme. The XPS spectra of Fe 2p region was presented in Fig. 3E, the peaks at 711.29 eV and 724.35 eV were attributed to the Fe 2p_{3/2} and Fe 2p_{1/2} binding energies, respectively. These results indicated the existence of Fe³⁺ and Fe²⁺ in CeFe-NCMzyme. The high-resolution peaks in the N1s spectrum of CeFe-NCMzyme can be fitted into two peaks at 400.53 eV and 398.29 eV (Fig. S3), which correspond to graphitic N and pyridinic N, respectively. Pyridinic N can improve the catalytic activity and stability of the catalysts [36]. Considering the XPS results, the synergistic effect of CeO₂, Fe₃O₄, and N-doped porous carbon materials can considerably enhance the enzyme-like catalytic activity of CeFe-NCMzyme. Based on the aforementioned results, a potential mechanism for the POD-like activity of CeFe-NCMzyme was proposed: First, a large amount of H₂O₂ was easily adsorbed onto CeFe-NCMzyme surface by oxygen vacancies via the pores. Ce³⁺ in CeFe-NCMzyme can react with H₂O₂ to generate Ce⁴⁺, and subsequently decompose H₂O₂ to produce ·OH under acidic conditions via a Fenton-like reaction. Meanwhile, H₂O₂ can easily obtain electrons from Fe²⁺ to produce ·OH and regenerate Fe³⁺. Fortunately, Ce⁴⁺ and Fe³⁺ can attract electrons from ·HO₂, leading to Fe³⁺/Fe²⁺ and Ce³⁺/Ce⁴⁺ redox recycles. Therefore, the redox cyclic catalytic reaction of Ce³⁺/Ce⁴⁺ and Fe³⁺/Fe²⁺ can be achieved, which cyclically decomposes H₂O₂ to produce ·OH (equations (3)–(7)).





The catalytic mechanism was further investigated using the electron paramagnetic resonance (EPR) experiment and the results were shown in Fig. 3F. A strong signal for the DMPO-hydroxyl radical ($\cdot\text{OH}$) was clearly observed, suggesting that CeFe-NCMzyme could catalyze H_2O_2 to generate $\cdot\text{OH}$ under acidic conditions through a Fenton-like reaction. To further confirm the presence of free radicals in CeFe-NCMzyme system, the scavengers of isopropanol ($\cdot\text{OH}$ scavenger), D-histidine ($^1\text{O}_2$ scavenger) and p-benzoquinone ($\cdot\text{O}_2$ scavenger) were added into CeFe-NCMzyme + TMB + H_2O_2 system. As shown in Fig. S4, D-histidine and p-benzoquinone exerted slight effect on the POD-like activity, whereas isopropanol exhibited considerable inhibition capability. These results indicated that the main free radical produced in the CeFe-NCMzyme system was $\cdot\text{OH}$. In conclusion, CeFe-NCMzyme possessed high POD-like activity owing to Fenton catalysis.

3.4. NOR detection using CeFe-NCMzyme

A previous study [37] demonstrated that the $-\text{SH}$ group of Cys can easily react with metal to form S-metal bonds, preventing electron transfer between metals. However, S-metal can be oxidized to $\text{S}=\text{O}$ by NOR, subsequently recovering the electron transfer between metals. Based on the prevention and recovery of electron transfer between metals using Cys and NOR, a colorimetric sensor based on CeFe-NCMzyme + TMB + H_2O_2 system was designed for the rapid and real-time determination of NOR in water samples. For obtaining an ideal limit of detection (LOD) and a wide linear detection range for NOR, the sensitivity of Cys in CeFe-NCMzyme sensor was first investigated. As shown in Fig. 4A, a

peak at 652 nm could be observed in CeFe-NCMzyme + H_2O_2 + TMB system. However, the peak intensity continuously decreased with increasing Cys concentration (Fig. 4B) and the blue colour gradually disappeared (Fig. 4B inset). Therefore, a linear relationship between the intensity of the peak at 652 nm and Cys concentrations was derived with the following equation of $y = -0.02364x + 1.2751$. The regression coefficient (R^2) reached 0.9880 in the linear range of 0.2–40.0 μM (Fig. 4C). The blue colour was almost disappeared at 40.0 μM (Fig. 4B). Therefore, 40.0 μM was adopted as the optimal Cys concentration for NOR detection using CeFe-NCMzyme system.

As presented in Fig. 4D, the intensity of the peak at 652 nm continuously increased along with increasing of NOR concentration in CeFe-NCMzyme + H_2O_2 + TMB + Cys system, and the solution colour clearly changed from colourless to blue (Fig. 4E inset). A calibration curve was constructed by measuring the absorbance (652 nm) at different NOR concentrations, and the regression equation was $y = 0.04241x + 0.3777$ ($R^2 = 0.9910$) within the range of 0.05–20.0 μM . The LOD was 35.70 nM based on $3\sigma/\text{slope}$ rule ($S/N = 3$) (Fig. 4F). Compared with other colorimetric methods (Table S2), the aforementioned strategy possessed more favourable characteristics for the rapid, highly sensitive, and visual detection of NOR. To further understand the applicability of the as-developed method for NOR detection, a possible mechanism was proposed based on the previous reports [37,38]. Because of the POD-like activity, the blue oxidized TMB (oxTMB) can be generated (considered as “on”) in CeFe-NCMzyme + H_2O_2 system. After the addition of Cys, S-metal bonds can be formed between the $-\text{SH}$ group of Cys and the metals (Ce and Fe) of CeFe-NCMzyme, which prevents the electron transfer in CeFe-NCMzyme and reduces the generation of $\cdot\text{OH}$, resulting in the inhibition of TMB oxidation (“off”). The S-metal group can be oxidized to form a $\text{S}=\text{O}$ bond by NOR, which can restore metal electron transfer. Therefore, TMB continues to be oxidized to form oxTMB with blue color restoration (“on”). In conclusion, the “on-off-on” effect of TMB oxidation was the mechanism underlying the usage of CeFe-NCMzyme as a colorimetric sensor for NOR detection.

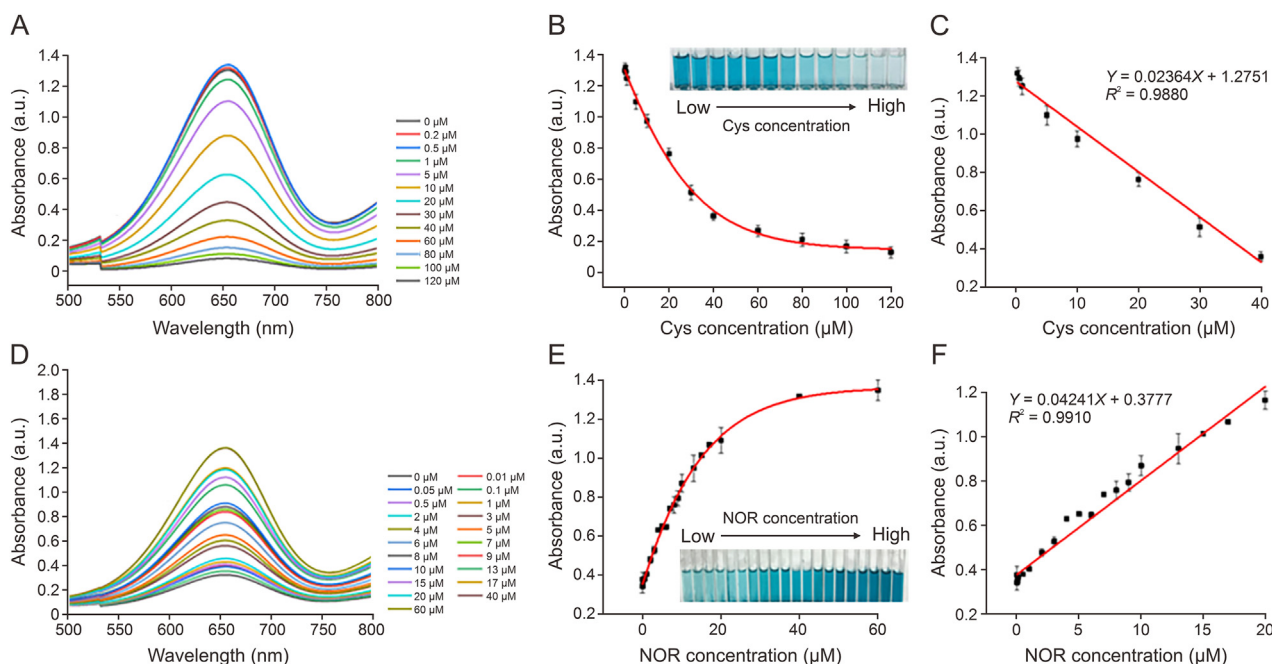


Fig. 4. Sensitivity to norfloxacin (NOR). (A, D) Absorption spectra of oxidative 3,3',5,5'-tetramethylbenzidine (oxTMB) at different concentrations of L-Cysteine (Cys) (A) and NOR (D). (B, E) Plot of the relationship between the concentrations of Cys (B) and NOR (E) at 652 nm. (C, F) Calibration curve for Cys (C) and NOR (F), respectively.

3.5. Selectivity, stability and repeatability of CeFe-NCMzyme

The selectivity of the prepared nanozyme toward Cys and NOR was studied via anti-interference experiments, in which the concentration of interferences was ten-folds higher than that of Cys and NOR, respectively. For the anti-interference of Cys, various amino acids (histidine, aspartic acid, alanine, and glycine) and metal ions (Na^+ , Ni^{2+} , Mg^{2+} , Mn^{2+} , SO_4^{2-} , Ca^{2+} , and Cl^-) were all added into CeFe-NCMzyme + H_2O_2 + TMB system. Obviously, after adding of anti-interferences, the peak at 652 nm was similar to that noted for the blank sample (Fig. 5A), indicating that the effects of these interferences on Cys could be ignored. To investigate the NOR selectivity of the prepared nanozyme, erythromycin, doxycycline, terramycin, alanine, histidine, aspartic acid, glycine, Mn^{2+} , Zn^{2+} , Na^+ , Ca^{2+} , and Ni^{2+} were used as interferences. As shown in Fig. 5B, these interferences exerted negligible effects on the adsorption peak at 652 nm, suggesting that CeFe-NCMzyme colorimetric sensor possessed good selectivity toward NOR. In addition, the interference of other quinolones, such as levofloxacin and ciprofloxacin, was investigated. As shown in Fig. S5, CeFe-NCMzyme colorimetric sensor showed a similar detection capability for levofloxacin and ciprofloxacin because of the similar structure of these quinolones, suggesting that this simple method can be used for the QN detection.

Furthermore, the long-term stability of CeFe-NCMzyme was also evaluated. The POD-like activity of CeFe-NCMzyme was detected every 5 d after storage for 60 d at room temperature. As shown in Fig. 5C, CeFe-NCMzyme possessed good stability because the POD-like activity remained above 95.00% after 60 day of storage. Additionally, the repeatability of CeFe-NCMzyme was evaluated and results were presented in Fig. 5D. Obviously, the POD-like activity was decreased by approximately 50.0% after four circles, which may be because the surface metal ions (Ce and Fe) were almost depleted in CeFe-NCMzyme + TMB + H_2O_2 system. However, CeFe-NCMzyme maintained a certain level of POD-like activity in TMB + H_2O_2 system after four circles due to the interior redox cyclic catalytic reaction of $\text{Ce}^{3+}/\text{Ce}^{4+}$ and $\text{Fe}^{3+}/\text{Fe}^{2+}$.

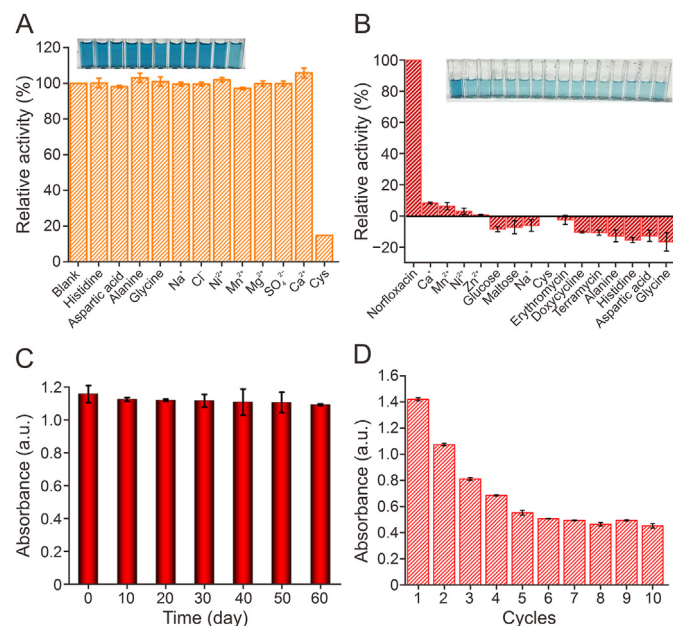


Fig. 5. Selectivity and stability of CeFe-NCMzyme. (A, B) Selectivity of CeFe-NCMzyme for L-Cysteine (Cys) (A) and norfloxacin (NOR) (B). (C) Stability of CeFe-NCMzyme. (D) Peroxidase (POD)-like activity of CeFe-NCMzyme after ten cycles.

3.6. Detection of NOR using POCT platform

To achieve on-site detection without delay, a quantitative POCT platform was developed by combining a smartphone with CeFe-NCMzyme by employing software ColorPicker App (Fig. 6A), which was used to capture the solution colour images and subsequently transfer into RGB values after the addition of NOR into CeFe-NCMzyme + TMB + H_2O_2 + Cys system (Fig. 6B). The colour of the solution gradually changed from colourless to blue with increasing NOR concentration. The linear relationship between the B/G ratio and NOR concentration was calculated and plotted. As shown in Fig. 6B, an excellent linear relationship was observed between NOR concentration and B/G values. The regression equation was $y = 0.00893x + 0.9964$ ($R^2 = 0.9700$) in the ranging of 0.1–20.0 μM , and the LOD of POCT platform was 54.10 nM based on the $3\sigma/s$. Clearly, the LOD of CeFe-NCMzyme colorimetric sensor and POCT platform were all within the limit of 21.0–420.9 μM recommended by the National Standards of China (GB 31656.3-2021), indicating that the POCT platform can be employed for the on-site visual detection of residual NOR in real samples.

3.7. Detection of NOR in real samples

To verify the applicability and practicality of the developed strategies, the spiked NOR in real water samples (Ganjing River, Poyang Lake, Tap water, and Purified water) was detected using CeFe-NCMzyme colorimetric sensor and POCT platform, respectively. As illustrated in Tables 1 and S3, the recoveries of all samples ranged from 90.20% to 108.00% with a relative standard deviation (RSD) <2.00% for the CeFe-NCMzyme colorimetric sensor (Table S3). The recoveries of POCT platform was obtained between 97.73% and 102.01% with an RSD of <1.50% (Table 1). These results indicated that the developed CeFe-NCMzyme colorimetric sensor and POCT platform had an acceptable accuracy for NOR detection in

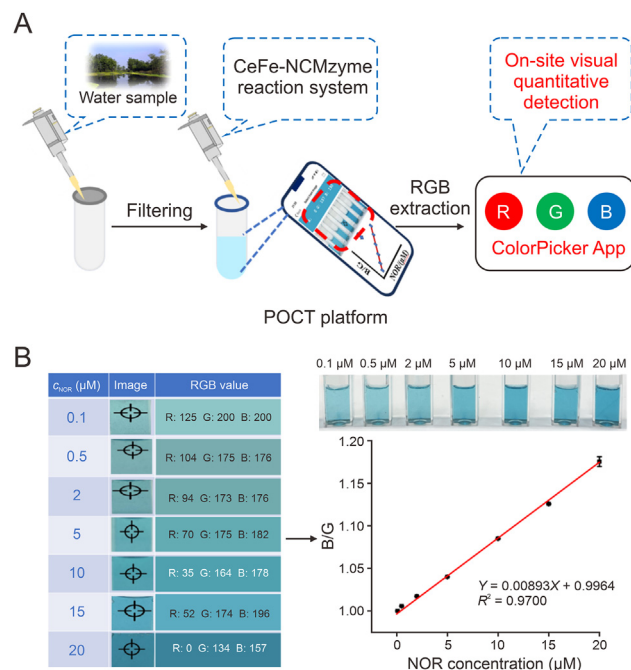




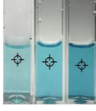

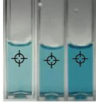


Fig. 6. Fabrication of point-of-care testing (POCT) platform. (A) POCT platform combination smartphone with CeFe-NCMzyme. (B) Sample photos and red, blue, and green (RGB) values of different spiked samples in CeFe-NCMzyme + 3,3',5,5'-tetramethylbenzidine (TMB) + H_2O_2 + L-Cysteine (Cys) system, and the corresponding quantification curves of B/G values via NOR concentrations. Cys: L-Cysteine.

Table 1
Images, RGB values, and recoveries of the spiking NOR in water samples using POCT platform.

Sample	Added (μM)	Images	RGB values	B/G values	Recovery (%)	RSD (%)
Ganjiang River	0.5		R: 113 G: 177 B: 176	0.998	99.72	0.33
	5		R: 64 G: 166 B: 173	1.040	99.92	0.28
	15		R: 0 G: 143 B: 162	1.131	100.07	0.38
Poyang Lake 1	0.5		R: 116 G: 167 B: 166	0.996	99.51	0.35
	5		R: 76 G: 158 B: 163	1.038	99.71	1.11
	15		R: 44 G: 167 B: 188	1.131	100.07	0.52
Poyang Lake 2	0.5		R: 104 G: 164 B: 164	1.000	99.92	0.60
	5		R: 72 G: 161 B: 168	1.043	100.00	0.078
	15		R: 61 G: 158 B: 174	1.105	97.73	0.70
Poyang Lake 3	0.5		R: 139 G: 191 B: 190	0.996	99.55	0.31
	5		R: 84 G: 180 B: 188	1.042	100.10	0.30
	15		R: 67 G: 176 B: 196	1.123	99.36	0.82
Poyang Lake 4	0.5		R: 140 G: 192 B: 194	1.005	100.43	0.91
	5		R: 94 G: 187 B: 195	1.040	99.91	0.25
	15		R: 50 G: 152 B: 167	1.106	97.81	0.70
Tap water	0.5		R: 128 G: 189 B: 188	0.998	99.72	0.65
	5		R: 44 G: 163 B: 173	1.062	102.01	0.059
	15		R: 0 G: 156 B: 174	1.123	99.36	1.46
Purified water	0.5		R: 120 G: 172 B: 171	0.998	99.73	0.64
	5		R: 76 G: 152 B: 158	1.039	99.82	0.067
	15		R: 2 G: 130 B: 144	1.117	98.84	1.37

RGB: red, blue, and green; NOR: norfloxacin; POCT: point-of-care testing; RSD: relative standard deviation.

real samples, exhibiting the features of cost-effectiveness, ease-to-use, portability, and reliability.

To further confirm the application of CeFe-NCMzyme colorimetric sensor and POCT platform in other real samples, studies were conducted using NOR capsules (100 mg, HAPHARM GROUP Co., Ltd., HarBin, China) and tablets (100 mg, The Central Pharmaceutical Co., Ltd., Tianjing, China) (Fig. 7A) as the real samples. The RGB values (Fig. 7B) and NOR contents were detected using CeFe-NCMzyme colorimetric sensor and POCT platform. The pretreatment processes for NOR in the capsules and tablets were provided in the [Supplementary data method](#). As depicted in Fig. 7C, the NOR

contents detected using the CeFe-NCMzyme colorimetric sensor, POCT, and traditional UV method was 99.27 mg, 99.74 mg, and 95.73 mg for capsules, and 87.13 mg, 87.05 mg, and 86.80 mg for tablets, respectively. These aforementioned findings indicated that CeFe-NCMzyme based methods can be used for the detection of other real samples.

4. Conclusions

In summary, a novel nanozyme (CeFe-NCMzyme) with a porous structure, large surface area, and carbon-based material properties was prepared. The POD-like activity of CeFe-NCMzyme was greatly enhanced compared with that of CeO₂ NPs or Fe₃O₄ NPs alone. The POD-like activity of CeFe-NCMzyme can be quenched by Cys and subsequently restored by the addition of NOR. Based on the 'on-off-on' model for POD-like activity, a CeFe-NCMzyme colorimetric sensor and POCT platform were developed for NOR detection. A wide linear detection range for 0.05–20.0 μM ($R^2 = 0.9910$) was obtained with a LOD of 35.70 nM for the colorimetric sensor. The recoveries of the water samples was ranged from 90.20% to 108.00% with an RSD of less than 2.00%. The POCT platform can be used for on-site visual quantification of NOR via RGB analysis. A linear range from 0.1 to 20.0 μM and a LOD of 54.10 nM were obtained for NOR, and the spiked recoveries were ranged from 97.73% to 102.01% with good accuracy and acceptable reliability. The LOD values of CeFe-

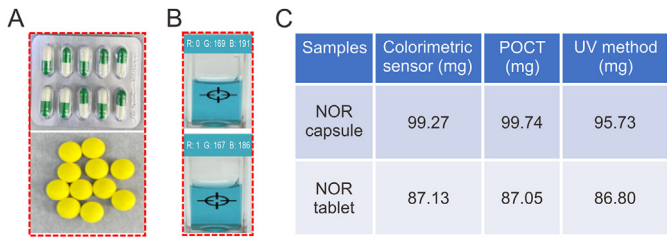


Fig. 7. Application of CeFe-NCMzyme colorimetric sensor and point-of-care testing (POCT) platform in other real samples. (A) Norfloxacin (NOR) capsule and tablet. (B) Red, blue, and green (RGB) values of capsule and tablet. (C) Norfloxacin (NOR) contents in capsule and tablet.

NCMzyme colorimetric sensor and POCT platform were within the limit of 21.0–420.9 μM recommended by the National Standards of China (GB 31656.3-2021). Therefore, the developed quantitative POCT system is useful for monitoring NOR contamination in water, particularly in resource-constrained areas.

CRedit authorship contribution statement

Yue Liu: Project administration, Methodology, Formal analysis, Conceptualization. **Taimei Cai:** Writing – original draft, Resources, Project administration, Funding acquisition. **Sen Chen:** Software, Methodology, Data curation. **Tao Wen:** Visualization, Validation, Software. **Hailong Peng:** Writing – review & editing, Supervision, Funding acquisition, Conceptualization.

Declaration of competing interest

The authors declare that there are no conflicts of interest.

Acknowledgments

This work was financially supported by Natural Science Foundation of Jiangxi Province (Grant Nos.: 20224ACB203016 and 20224BAB203022), Science and Technology Research Project of Jiangxi Provincial Department of Education (Grant No.: GJJ2201322), the National Natural Science Foundation of China (Grant Nos.: 32060577 and 32360619), and Natural Science Foundation for Distinguished Young Scholars of Hunan Province (Grant No.: 2023JJ10099).

Appendix A. Supplementary data

Supplementary data to this article can be found online at <https://doi.org/10.1016/j.jpha.2024.101023>.

References

- J. Yan, R. Hu, Z. Lin, et al., pH-regulated terbium(III) infinite coordination polymer sensor array for pattern discrimination of quinolone antibiotics, *ACS Appl. Opt. Mater.* 1 (2023) 209–215.
- Y. Wu, J. Xiong, S. Wei, et al., Molecularly imprinted polymers by reflux precipitation polymerization for selective solid-phase extraction of quinolone antibiotics from urine, *J. Chromatogr. A* 1714 (2024), 464550.
- Y. Zhu, P. He, H. Hu, et al., Determination of quinolone antibiotics in environmental water using automatic solid-phase extraction and isotope dilution ultra-performance liquid chromatography tandem mass spectrometry, *J. Chromatogr. B Anal. Technol. Biomed. Life Sci.* 1208 (2022), 123390.
- G. van Vyncht, A. János, G. Bordin, et al., Multiresidue determination of (fluoro)quinolone antibiotics in swine kidney using liquid chromatography-tandem mass spectrometry, *J. Chromatogr. A* 952 (2002) 121–129.
- S. Bang Ye, Y. Huang, D.Y. Lin, QuEChERS sample pre-processing with UPLC-MS/MS: A method for detecting 19 quinolone-based veterinary drugs in goat's milk, *Food Chem* 373 (2022), 131466.
- A.O. Melekchin, V.V. Tolmacheva, N.O. Goncharov, et al., Rapid multi-residue LC-MS/MS determination of nitrofurantol metabolites, nitroimidazoles, amphenicols, and quinolones in honey with ultrasonic-assisted derivatization - magnetic solid-phase extraction, *J. Pharm. Biomed. Anal.* 237 (2024), 115764.
- S.G. Dmitrienko, E.V. Kochuk, V.V. Apyari, et al., Recent advances in sample preparation techniques and methods of sulfonamides detection - A review, *Anal. Chim. Acta* 850 (2014) 6–25.
- G. Xing, J. Ai, N. Wang, et al., Recent progress of smartphone-assisted microfluidic sensors for point of care testing, *Trac Trends Anal. Chem.* 157 (2022), 116792.
- J. Liu, Z. Geng, Z. Fan, et al., Point-of-care testing based on smartphone: The Current state-of-the-art (2017-2018), *Biosens. Bioelectron.* 132 (2019) 17–37.
- H.N. Chan, M.J.A. Tan, H. Wu, Point-of-care testing: Applications of 3D printing, *Lab Chip* 17 (2017) 2713–2739.
- X. Lin, M. Zhao, T. Peng, et al., Detection and discrimination of pathogenic bacteria with nanomaterials-based optical biosensors: A review, *Food Chem.* 426 (2023), 136578.
- J. Xu, C. Liang, Z. Gao, et al., Construction of nanoreactors on TiO_2 nanotube arrays as a POCT device for sensitive colorimetric detection, *Chin. Chem. Lett.* 34 (2023), 107863.
- Y. Shen, Y. Wei, Z. Liu, et al., Engineering of 2D artificial nanozyme-based blocking effect-triggered colorimetric sensor for onsite visual assay of residual tetracycline in milk, *Mikrochim. Acta* 189 (2022), 233.
- J. Zhang, J. Qian, Q. Mei, et al., Imaging-based fluorescent sensing platform for quantitative monitoring and visualizing of fluoride ions with dual-emission quantum dots hybrid, *Biosens. Bioelectron.* 128 (2019) 61–67.
- L. Guo, S. Chen, Y. Yu, et al., A smartphone optical device for point-of-care testing of glucose and cholesterol using Ag NPs/ $\text{UiO}-66-\text{NH}_2$ -based ratio-metric fluorescent probe, *Anal. Chem.* 93 (2021) 16240–16247.
- M. Zhang, X. Cui, N. Li, Smartphone-based mobile biosensors for the point-of-care testing of human metabolites, *Mater. Today Bio* 14 (2022), 100254.
- L. Wang, Y. Cui, Y. Mi, et al., The fabrication of quantum dots microgel based POCT microfluidic chip for simultaneously detecting multiple pathogenic heavy metal ions and its applications in actual water samples, *Microchem. J.* 199 (2024), 110089.
- A. Parihar, N.K. Choudhary, P. Sharma, et al., Carbon nanomaterials-based electrochemical aptasensor for point-of-care diagnostics of cancer biomarkers, *Mater. Today Chem.* 30 (2023), 101499.
- Z. Tan, H. Shi, Y. Zheng, et al., A 3D homogeneous microreactor with high mixing intensity at wide Re range for MOF preparation and POCT application, *Chem. Eng. J.* 476 (2023), 146481.
- R. Wang, Y. Du, Y. Fu, et al., Ceria-based nanozymes in point-of-care diagnosis: An emerging futuristic approach for biosensing, *ACS Sens.* 8 (2023) 4442–4467.
- K. Wang, X. Meng, X. Yan, et al., Nanozyme-based point-of-care testing: Revolutionizing environmental pollutant detection with high efficiency and low cost, *Nano Today* 54 (2024), 102145.
- L. Zhang, X. Bi, X. Liu, et al., Advances in the application of metal-organic framework nanozymes in colorimetric sensing of heavy metal ions, *Nanoscale* 15 (2023) 12853–12867.
- C. Lou, F. Yang, L. Zhu, et al., Dual-function sensor based on $\text{NH}_2\text{-MIL}-101(\text{Fe})/\text{Cu}/\text{CeO}_2$ nanozyme for colorimetric and fluorescence detection of heavy metals, *Colloids Surf. A Physicochem. Eng. Aspects* 677 (2023), 132398.
- S. Cao, B. Zou, J. Yang, et al., Hollow $\text{CuO}-\text{CeO}_2$ nanospheres for an effectively catalytic annulation/ A^3 -coupling reaction sequence, *ACS Appl. Nano Mater.* 5 (2022) 11689–11698.
- P. Gai, L. Pu, C. Wang, et al., CeO_2/NC nanozyme with robust dephosphorylation ability of phosphotriester: A simple colorimetric assay for rapid and selective detection of paraoxon, *Biosens. Bioelectron.* 220 (2023), 114841.
- Z. Tong, J. Sha, D. Liu, et al., An unprecedented $\text{FeMo}_6/\text{Ce-UiO}-66$ nanocomposite with cascade enzyme-mimic activity as colorimetric sensing platform, *Chemistry* 28 (2022), e202104213.
- T. Cai, L. Yao, J. Fan, et al., Fe-Ni bimetallic nanoparticles encapsulated into nanofibrous carbon microspheres as a catalytic nanoreactor for highly selective hydrogenation of 5-hydroxymethylfurfural to 2, 5-dihydroxymethylfuran or 2, 5-dihydroxymethyltetrahydrofuran, *J. Taiwan Inst. Chem. Eng.* 146 (2023), 104870.
- R. Nie, H. Yang, H. Zhang, et al., Mild-temperature hydrodeoxygenation of vanillin over porous nitrogen-doped carbon black supported nickel nanoparticles, *Green Chem.* 19 (2017) 3126–3134.
- H. Wang, J. Shang, Z. Xiao, et al., Novel construction of carbon bonds in CeO_2/C with efficiently photocatalytic activity, *Dyes Pigm.* 182 (2020), 108669.
- F. Cheng, S. Wang, H. Zheng, et al., Cu-doped cerium oxide-based nanomedicine for tumor microenvironment-stimulative chemo-chemodynamic therapy with minimal side effects, *Colloids Surf. B Biointerfaces* 205 (2021), 111878.
- S. Wang, J. Long, T. Jiang, et al., Magnetic $\text{Fe}_3\text{O}_4/\text{CeO}_2/\text{g-C}_3\text{N}_4$ composites with a visible-light response as a high efficiency Fenton photocatalyst to synergistically degrade tetracycline, *Sep. Purif. Technol.* 278 (2021), 119609.
- Z. Xiao, X. Wu, H. Tan, et al., Design and synthesis of Fe-Ce-O/C with efficient photocatalytic activity, *J. Rare Earths* 41 (2023) 91–99.
- Y. Xia, F. Shi, R. Liu, et al., *In situ* electrospinning MOF-derived highly dispersed α -cobalt confined in nitrogen-doped carbon nanofibers nanozyme for biomolecule monitoring, *Anal. Chem.* 96 (2024) 1345–1353.
- D. Jampaiah, T. Srinivasa Reddy, A.E. Kandjani, et al., Fe-doped CeO_2 nanorods for enhanced peroxidase-like activity and their application towards glucose detection, *J. Mater. Chem. B* 4 (2016) 3874–3885.
- G. Liu, G. Hou, X. Mao, et al., Rational design of $\text{CeO}_2/\text{Bi}_2\text{O}_3$ flower-like nanosphere with Z-scheme heterojunction and oxygen vacancy for enhancing photocatalytic activity, *Chem. Eng. J.* 431 (2022), 133254.
- H. Miao, S. Li, Z. Wang, et al., Enhancing the pyridinic N content of Nitrogen-doped graphene and improving its catalytic activity for oxygen reduction reaction, *Int. J. Hydrog. Energy* 42 (2017) 28298–28308.
- S. Jiang, G. Su, J. Wu, et al., $\text{Co}_3\text{O}_4/\text{CoFe}_2\text{O}_4$ hollow nanocube multifunctional nanozyme with oxygen vacancies for deep-learning-assisted smartphone biosensing and organic pollutant degradation, *ACS Appl. Mater. Interfaces* 15 (2023) 11787–11801.
- S. Ye, S. Chen, T. Cai, et al., Iron-driven self-assembly of dopamine into dumbbell-shaped nanozyme for visual and rapid detection of norfloxacin on a smartphone-assisted platform, *Talanta* 274 (2024), 126003.